Published in final edited form as:
Nanoscale. 2013 November 21; 5(22): . doi:10.1039/c3nr03250g.

Aqueous Self-Assembly of Poly(ethylene oxide)-block-Poly(ε-caprolactone) (PEO-*b*-PCL) Copolymers: Disparate Diblock Copolymer Compositions Give Rise to Nano- and Meso-Scale Bilayered Vesicles†

Wei Qi[a,b], **P. Peter Ghoroghchian**[c], **Guizhi Li**[b], **Daniel A. Hammer**[d], and **Michael J. Therien**[a,*]

[a]Department of Chemistry, French Family Science Center, 124 Science Drive, Duke University, Durham, North Carolina 27708, USA

[b]Department of Chemistry, 231 South 34th Street, University of Pennsylvania, Philadelphia, Pennsylvania 19104,USA

[c]Dana Farber Cancer Institute, 450 Brookline Avenue, Boston MA, 02115, USA

[d]Department of Bioengineering. School of Engineering and Applied Science, University of Pennsylvania, 3320 Smith Walk, Philadelphia, Pennsylvania 19104, USA

Abstract

Nanoparticles formed from diblock copolymers of FDA approved PEO and PCL have generated considerable interest as *in vivo* drug delivery vehicles. Herein, we report the synthesis of the most extensive family PEO-*b*-PCL copolymers that vary over the largest range of number-average molecular weights (M_n: 3.6 – 57K), PEO weight fractions (f_{PEO}: 0.08 – 0.33), and PEO chain lengths (0.75–5.8K) reported to date. These polymers were synthesized in order to establish the full range of aqueous phase behaviours of these diblock copolymers and to specifically identify formulations that were able to generate bilayered vesicles (polymersomes). Cryogenic transmission electron microscopy (cryo-TEM) was utilized in order to visualize the morphology of these structures upon aqueous self-assembly of dry polymer films. Nanoscale polymersomes were formed from PEO-*b*-PCL copolymers over a wide range of PEO weight fractions (f_{PEO}: 0.14 – 0.27) and PEO molecular weights (0.75 – 3.8K) after extrusion of aqueous suspensions. Comparative morphology diagrams, which describe the nature of self-assembled structures as a function of diblock copolymer molecular weight and PEO weight fraction, show that in contrast to micron-scale polymersomes, which form only from a limited range of PEO-*b*-PCL diblock copolymer compositions, a multiplicity of PEO-*b*-PCL diblock copolymer compositions are able to give rise to nanoscale vesicles. These data underscore that PEO-*b*-PCL compositions that spontaneously form micron-sized polymersomes, as well as those that have previously been reported to form polymersomes via a cosolvent fabrication system, provide only limited insights into the distribution of PEO-*b*-PCL diblocks that give rise to nanoscale vesicles. The broad range of polymersome-forming PEO-*b*-PCL compositions described herein suggest the ability to construct extensive families of nanoscale vesicles of varied bilayer thickness, providing the ability to tune the timescales of vesicle degradation and encapsulant release based on the intended *in vivo* application.

†Electronic Supplementary Information (ESI) available: [materials and methods, characterization data]. See DOI: 10.1039/b000000x/

michael.therien@duke.edu; Phone: +1 919 660 1670; Fax: +1 919 684 1522.

Introduction

Polymersomes (50 nm – 50 μm diameter polymer vesicles) formed from amphiphilic block copolymers have attracted much attention due to their superior mechanical stabilities and chemical properties relative to those of conventional lipid-based vesicles (liposomes) and micelles.[1–5] Polymer vesicles can readily encapsulate water-soluble hydrophilic compounds (drugs, vitamins, fluorophores, etc.) inside of their aqueous cavities, but also have been shown to be capable of encapsulating large hydrophobic molecules[5–9] within their thick lamellar membranes. Moreover, the sizes, membrane thicknesses, and stabilities of these synthetic vesicle assemblies can be rationally tuned via various preparative methods[3, 4] that modulate block copolymer chemical structure, number-average molecular weight, and the ratio of hydrophilic to hydrophobic volume fractions, giving rise to polymersomes with varied characteristics that that may be optimized for applications in medical imaging, drug delivery, and for topical cosmetic purposes.[3, 5, 10]

To date, polymersomes have been formed predominantly from amphiphilic diblock copolymers that include poly(ethylene oxide)-*b*-poly(butadiene) (PEO-*b*-PBD),[2, 3, 5] poly(ethylene oxide)-*b*-poly(ethylethylene) (PEO-*b*-PEE),[2] poly(styrene)-*b*-poly(ethylene oxide) (PS-*b*-PEO),[11–13] poly(styrene)-*b*-poly(acrylic acid) (PS-*b*-PAA),[3, 11, 14] poly(ethylene oxide)-*b*-poly(propylenesulfide) (PEO-PPS),[15–17] poly(2-(methacryloyloxy)-ethylphosphoryl-choline)-*b*-poly(2-(diisopropylamino)ethylmethacrylate) (PMPC-PDPA),[18, 19] and poly(styrene)-*b*-poly(isocyanoalanine) (2-thiophene-3-ylethyl) amide (PS-PIAT).[20–23] None of these well-established polymersome formulations, however, generates fully biodegradable vesicles via aqueous self-assembly. A few biodegradable polymersome compositions have been prepared from amphiphilic diblock copolymers of PEO and aliphatic polyesters/polycarbonates using an organic co-solvent/water injection/extraction method.[24–26] In contrast to polymersome preparative procedures based on self-assembly (*i.e.*, film hydration, bulk hydration, or electroformation), the co-solvent method requires the organic co-solvent to be completely removed from the aqueous polymersome suspension post-assembly.

We have previously reported the generation of polymersomes via thin-film hydration of the diblock copolymer PEO(2K)-*b*-PCL(12K);[27] the biomedical utility of PEO-*b*-PCL diblock copolymers is noteworthy in that they contain two previously FDA-approved building blocks, poly(ethylene oxide) (PEO) and poly(ε-caprolactone) (PCL). Unlike degradable polymersomes formed from blending "bio-inert" and hydrolysable components,[28, 29] PEO-*b*-PCL-based vesicles are fully bioresorbable,[30] leaving no potentially toxic byproducts upon their degradation. In contrast to other degradable (polypeptide-, polyester-, or polyanhydride-based) polymersomes,[24, 25, 31–33] PEO(2K)-*b*-PCL(12K)-based vesicles are formed through spontaneous self-assembly of the pure amphiphilic diblock copolymer, offering manufacturing advantages in terms of cost and safety. Further, these fully bioresorbable polymersomes possess *in vivo* drug release kinetics appropriate for potential intravascular drug delivery applications.[27]

It is well known that particle sizes greatly influence blood circulation times, reticuloendothelial system (RES) recognition, biodistribution, and the mechanisms of cell uptake.[34–36] The *in vivo* uptake of particles and their extent of drug release increase with decreasing particle sizes and increasing particle surface-area-to-volume ratios.[37–39] As the optimal particle size for prolonged blood stream circulation is ~80–150 nm, and the intracellular uptake of particles having diameters larger than 1 μm is minimal,[37–39] nanometer-sized bioresorbable vesicles are critical for *in vivo* drug delivery of encapsulated therapeutics. Congruent with these requirements, Butler and coworkers[25] have further examined the formation of nano-sized vesicles from a handful of commercially available

PEO-*b*-PCL block copolymer compositions featuring mostly small PEO chain lengths (300–2000) and low copolymer molecular weights (M_w: 2.6–7.8K) by the co-solvent injection method.[25]

Expanding upon our initial work,[27] as well as the studies by Butler and colleagues,[25] we describe herein the development of an extensive family of amphiphilic poly(ethylene oxide)-*b*-polycaprolactone (PEO-*b*-PCL) diblock copolymers with varying hydrophilic PEO block weight fractions (f_{PEO}: 0.08 – 0.33) and PEO chain lengths (0.75 – 5.8K); we further screened their ability to assemble into bilayered vesicles through aqueous self-assembly of their respective dry polymer films deposited on Teflon™. These biodegradable PEO-*b*-PCL diblock copolymers were fabricated by: (i) ring-opening polymerization of ε-caprolactone monomer (ε-CL) followed by coupling to commercially available monomethoxyl PEO (MePEO), and (ii) sequential anionic living polymerization of PEO and ε-CL monomers. The synthesized PEO-*b*-PCL diblock copolymers possessed number-average molecular weights spanning 3.6 – 57 K, PEO block weight fractions ranging from 0.08 – 0.33, and polydispersity indices (PDIs) ranging between 1.14 and 1.37 (Electronic Supplementary Information, ESI). The generated morphologies of PEO-*b*-PCL copolymers prepared via self-assembled thin-film rehydration techniques were examined. Comparative morphology diagrams that describe the nature of self-assembled structures as a function of diblock copolymer molecular weight and PEO weight fraction exhibit dramatic differences for the nano- and meso-scale size domains. These studies demonstrate that in contrast to the single diblock copolymer formulation of PEO(2K)-*b*-PCL(12K) (PDI = 1.21) that produces quantitatively micron-sized polymersomes, nanoscale polymersomes can be formed from a multiplicity of PEO-*b*-PCL diblock copolymer compositions under thin-film rehydration conditions.

Experimental

Polymersome Preparation

The thin-film hydration method was employed to assemble the PEO-*b*-PCL copolymers into their equilibrium aqueous morphologies. Thin-film hydration has been extensively utilized for preparing non-biodegradable polymersomes comprised of PEO-*b*-PBD diblock copolymers via aqueous self-assembly;[5] an analogous protocol was employed herein for experiments involving PEO-*b*-PCL copolymers. An organic solution containing the dissolved biodegradable polymer (200 μl of 7 mg/mL polymer in $CHCl_3$) was uniformly coated on the surface of a roughened Teflon™ plate followed by vacuum evaporation for > 12 h. Addition of an aqueous solution (*e.g.*, DI water) and heating at 60 °C for 48 h led to spontaneous budding of giant (5 – 20 μm) biodegradable polymersomes into suspension. In polymersome samples that contained 1 mol% Nile red, the dye was incorporated into the hydrophobic vesicle bilayer during the self-assembly process noted above, which enabled facile visualization of resultant copolymer aqueous morphology via confocal fluorescence microscopy (ESI). Nanoscale unilamellar polymersomes were prepared via procedures analogous to those used to formulate small lipid vesicles (sonication, freeze-thaw extraction and extrusion). The sonication procedure involved placing a sample vial containing the aqueous-based solution and a dried thin-film formulation (of polymer uniformly deposited on Teflon™) into a bath sonicator (Fischer Scientific; Model FS20) with constant agitation for 2 h. Freeze-thaw extraction cycles (10) were carried out by alternatively placing the sample vials in liquid N_2 and warm water baths. A narrow size distribution of nano-sized polymersomes was achieved with 3 extrusions using a Liposofast Basic hand-held extruder equipped with 400 nm polycarbonate membranes (Avestin Inc., Ottawa, Ontario). These nano-sized polymersomes were lyophilized and subject to chromatographic purification (PLgel 5μm mixed C, 300 × 7.5 mm, linear MW operating range: 200–2,000,000 g/mol) in

order to verify that no measurable PCL hydrolysis of the PEO-*b*-PCL polymers occurred under these experimental conditions.

Results and discussion

Synthesis and Characterization of Biodegradable PEO-*b*-PCL Diblock Copolymers

A series of PEO-*b*-PCL diblock copolymers (Table 1) were synthesized (ESI) via ring-opening polymerization of ε-CL and commercially available MePEO (M_n = 5000, 2000, 1100 and 750). MePEO homopolymers bearing one hydroxyl end group were used as the macroinitiator to activate polymerization (130 °C, 24 h) of ε-CL monomer in the presence of catalyst (tin octanoate, $SnOct_2$). PEO-*b*-PCL diblock copolymers have been previously synthesized under a variety of catalyzed[24, 40–42] and non-catalyzed conditons.[43, 44] Non-catalyzed ring-opening polymerization of ε-CL must, however, be carried out ≥180 °C over several days, which is cumbersome. Of the previously established catalysts, $SnOct_2$ is the most widely used for the production of biodegradable polyesters, as it is commercially available, easy to handle, soluble in common organic solvents and neat liquids (e.g., cyclic ester monomers), and is a permitted food additive in numerous countries.[45–48]

Although the synthesis of PEO-*b*-PCL copolymers from MePEO via ring-opening polymerization of ε-CL is facile, the availability of MePEO homopolymers is limited. As such, we utilized anionic living polymerization of ethylene oxide monomers to produce PEOs over an expansive range of molecular weights (M_w); subsequent ε-CL polymerization yields PEO-*b*-PCL copolymers that vary over the largest range of number-average molecular weights (M_n: 3.6 – 57K) and PEO weight fractions (f_{PEO}: 0.08 – 0.33) reported to date. An additional advantage of this approach is that the functionality of the PEO terminus of the PEO-*b*-PCL copolymer can be easily varied (ESI, Scheme S2). These ethylene oxide polymerization reactions utilized cyanomethyl potassium as the protected initiator, which was prepared by metalation of acetonitrile with potassium naphthalenide in THF.[49–52] While anionic living polymerization had been utilized previously in the syntheses of low molecular weight, high PEO weight fraction PEO-*b*-PCL copolymers [e.g., PEO(2.2K)-*b*-PCL(1.2K)],[52] this strategy, as presented herein, also provides PEO-*b*-PCL copolymers that possess a larger range of PEO block molecular weights (1.5, 2.6, 3.0, 3.8, and 5.8 KDa), low PEO weight fractions (f_{PEO}: 0.10 – 0.23), and a wider range of diblock M_n (7.8 – 47K) than has been explored previously. ^{1}H NMR spectroscopy was utilized to characterize the number-average molecular weight of the PEO homopolymers and the corresponding PEO-*b*-PCL diblock copolymers (ESI).[24, 40–44, 50] GPC was employed to characterize the molecular weight (M_w) and molecular weight distribution (M_w/M_n) (PDI) of each PEO-*b*-PCL diblock copolymer formulation (see ESI). GPC data indicate that PEO-*b*-PCL diblock copolymers synthesized by anionic living polymerization, having PEO molecular weights of 2.6, 3, 3.8 and 5.8K, exhibited the narrowest molecular weight distributions (PDI: 1.2 – 1.27). PEO-*b*-PCL diblock copolymers synthesized from PEO(2K) via ring-opening polymerization showed narrow molecular weight distributions (PDI: 1.1 – 1.2), while copolymers derived from PEO(5K) displayed distributions that were slightly wider (PDI: 1.32 – 1.37). These data establish that anionic living polymerization provides an excellent route for the synthesis of PEO-*b*-PCL diblock copolymers with controlled PEO chain length, modulated PEO/PCL block ratio, and narrow molecular weight distribution (see ESI).

Aqueous Morphologies of Meso-Scale PEO-*b*-PCL Diblock Copolymers

The thin-film hydration method was preferentially utilized to assemble meso-scale amphiphilic PEO-*b*-PCL diblock copolymers into their equilibrium aqueous morphologies (ESI, Table 1).[53] Data compiled in Table 1 describe the observed aqueous morphologies for the comprehensive set of PEO-*b*-PCL diblock copolymers that were fabricated; note that

extensive microscopy studies (confocal, TEM) demonstrate that preparations of micron-sized polymersomes gave rise to no measurable quantity of corresponding nanoscale structures.

Large numbers of meso-scale polymersomes were obtained from aqueous hydration and self-assembly of the PEO(2K)-*b*-PCL(12K) diblock copolymer (f_{PEO} = 0.14) (ESI, Fig. S3). These polymersomes possessed both multilamellar and unilamellar bilayered structures. In contrast, micron-sized polymersomes were found to coexist with irregular particles in aqueous preparations of PEO(2–3.8K)-*b*-PCL(9.5–22.2K) diblock copolymers, where f_{PEO} ranges between 0.12 and 0.19. In aqueous suspensions of PEO-*b*-PCL diblock copolymers derived from higher (5K or 5.8K) or lower (750 – 1.5K) molecular weight PEO blocks, no polymersomes were observed regardless of the PEO/PCL ratio (Fig. 1). Unlike conventional vesicle-generating PEO-*b*-PBD copolymers that have a broad range of compositions compatible with high yields of self-assembled meso-scale vesicles, the range of the PEO weight fraction (f_{PEO}: 0.12 – 0.19), PEO block size (2 – 3.8K), and total diblock M_n (1.5 – 26K) compatible with meso-scale polymersome formation for PEO-*b*-PCL diblock copolymers is relatively narrow (Fig. 1). The reduced PEO weight fractions of these polymersome-forming PEO-*b*-PCL compositions (f_{PEO} = 0.14) contrast sharply to the PEO-*b*-poly(ethylethylene) and PEO-*b*-poly(butadiene) diblock formulations that give rise to the archetypal polymersomal structure (f_{PEO}: 0.28 – 0.39),[4, 54]. The lower PEO weight fractions necessary to generate PCL-, and related biodegradable copolymer-, based polymersomes may be related to the higher phase transition temperatures for these compositions.[27, 55]

Note, in this regard Discher and coworkers have also studied the meso-scale morphologies generated from a series of PEO-*b*-PCL diblock copolymers using organic co-solvent evaporation;[53] their work focused upon polymeric compositions that featured PEO/PCL ratios that enabled the formation of worm-like micelles; their results, however, differ from those obtained with the experiments carried out with the broader selection of PEO-*b*-PCL diblock compositions examined herein, which describe f_{PEO}, PEO block size, and total diblock M_n ranges that give rise to meso-scale polymersomal morphologies. Note, for example, that the PEO(2K)-*b*-PCL(12K) diblock copolymer composition forms largely worm-like structures via the solvent evaporation method,[53] but quantitatively self-assembles into vesicles via thin-film hydration (Fig. 1). Likewise, (i) PEO(5K)-b-PCL(10K) forms vesicles and spheres via solvent evaporation,[53] but self-assembles into microspheres via the thin-film hydration method (Fig. S4), and (ii) PEO(5.8K)-*b*-PCL(24K), which has been previously shown to form meso-scale vesicles via solvent injection,[24] yields no polymersomes by thin-film hydration. These data indicate that the aqueous morphologies of PEO-*b*-PCL copolymers are sensitive to preparative method and experimental conditions, which may alter the local arrangement of polymer chains that form corresponding aqueous structures. In this regard, the organic co-solvent water injection/extraction method is well known to produce kinetically trapped morphologies that are sensitive to the order of addition, concentrations and ratios of copolymer and solvent, as well as the injection flow rate.[56]

In order to elucidate the effects of diblock copolymer molecular weight distribution on vesicle formation, PEO-*b*-PCL 3.8K) and narrow molecular distributions (PDI = 1.1) were separated by GPC; no further improvement in the yield of vesicles from these samples was observed relative to PEO-*b*-PCL diblock copolymers of the same molecular weight having slightly broader molecular weight distributions (PDI: 1.2 – 1.4). Similarly, the ability of PEO-*b*-PCL diblock copolymer mixtures having much wider molecular weight distributions were examined; scanning laser confocal microscopy of such samples (Fig. 2), shows that polymersomes can be obtained in high yield from a 1:1:1 PEO(2k)-*b*-PCL(9.5k):PEO(2k)-*b*-PCL(12k):PEO(2k)-*b*-PCL(15k) copolymer blend, suggesting that the molecular weight

distribution has little influence on biodegradable polymersome formation from mixtures containing a significant weight fraction of the PEO(2K)-b-PCL(12K) diblock copolymer.

Nanoscale Morphologies of Self-Assembled PEO-*b*-PCL Diblock Copolymers in Aqueous Suspension

Nanoscale polymersomes are formed from dry thin-films of PEO-*b*-PCL deposited on Teflon™ upon rehydration in an aqueous solution, along with the addition of sonic energy; several subsequent cycles of freeze/thaw extraction and extrusion (Figs. 3–4; see Experimental Section, ESI) yield vesicles of a desired size with narrow distribution (e.g. d ~100 +/− 15 nm). Solution morphologies were characterized utilizing cryo-TEM, which allowed for direct visualization of the aggregate nano-sized structures formed in aqueous suspension (Table 1); note that dynamic light scattering (DLS) measurements confirmed the homogeneous size distributions and were consistent with cryo-TEM experimental data. Nanoscale polymersomes are formed from PEO-*b*-PCL diblock copolymers of a range of PEO weight fractions (f_{PEO}: 0.14 – 0.27) and block sizes (PEO 0.75 – 3.8K). Butler et al.[25] examined a few low molecular weight PEO-*b*-PCL copolymers that assembled into nm-sized morphologies via co-solvent injection; the results of these investigators mirror the Table 1 data for low molecular weight PEO-*b*-PCL polymers (f_{PEO}: 0.14 – 0.27 and PEO molecular weights of 0.75 – 3.8K) that form nanoscale vesicles via self-assembly after thin-film hydration. Note, however, for high molecular weight PEO-*b*-PCL copolymers with PEO block molecular weight over 3.8K, such as PEO(5K, 5.8K)-PCL diblock copolymers, only spherical micelles and particles are formed under thin-film hydration conditions over a large range of PEO weight fractions (f_{PEO}: 0.09 – 0.33). It is important to underscore that significant morphological differences are evident for self-assembled meso- and nanoscale structures for a given PEO-*b*-PCL diblock copolymer. In contrast to morphologies generated on the meso scale, polymersomes dominate observed self-assembled nanoscale morphologies of these PEO-*b*-PCL diblock copolymers, suggesting disparate formation mechanisms for nano- and meso-sized polymersomes that form under thin film hydration conditions.

As shown in Fig. 5, both hydrophilic volume fraction and PEO chain length affect the observed distribution of self-assembled morphologies on the nanoscale. To further explore this issue, several PEO-*b*-PCL diblock copolymers were generated that featured the same PEO chain length (2K) but which differed with respect to hydrophilic PEO weight fraction (see **OCL 1–6** in Fig. 3); further, other PEO-*b*-PCL copolymers were also synthesized that exhibited identical PEO weight fractions, but which differed with respect to PEO chain length (see **OCL A–E** in Fig. 4). The data chronicled in Fig. 3 demonstrate that increasing the molecular weight of the PCL block at a constant PEO chain length (f_{PEO}: 0.21 → 0.08) results in a morphological transition from bilayered vesicles to micellar aggregates. Increasing the length of PCL block augments the hydrophobic content of the amphiphile while decreasing the interfacial curvature, leading to the development of micellar morphologies. Fig. 4 highlights that uniform spherical vesicles are formed from PEO(2K)-*b*-PCL diblock copolymers when $0.21 < f_{PEO} < 0.12$, with micelles first appearing when f_{PEO} falls below 0.14. For PEO-*b*-PCL diblock copolymers with f_{PEO} fixed at ~15%, PEO chain lengths ranging from 1.1 to 3.8K support polymersome formation at the nanoscale, while micellar aggregates are evident for diblocks having PEO molecular weights < 1.1K or > 3K.

It is well known that the morphology of diblock copolymer assemblies is determined by the interfacial curvature of the amphiphile;[52] moreover, previous work has revealed that the surface elasticity of bilayer membranes is scale independent and only depends on the interface.[4, 57] It is the expectation, therefore, that self-assembled diblock copolymer morphologies elucidated at one size domain provide predictive insights into morphologies

that will be evident over other size domains. While this has shown to be true for meso-scale and larger bilayered vesicles, these data emphasize that it is incorrect to extend such predictions to the nanoscale. While the origin of this effect can only be discussed qualitatively, it is likely that the dramatically increased total surface areas and correspondingly decreased surface tensions characteristic of nanoscale bilayered vesicles serve to mitigate destabilizing effects that derive from the augmented interfacial curvature required for vesicle formation, relative to hypothetical micron-sized vesicles derived from an identical diblock copolymer. Likewise, this observed difference in ability to form mesoscopic versus nanoscopic vesicles may stem in part from the crystallinity of the hydrophobic PCL chains.[30] The restricted mobility of the PCL chains may allow the assembly of small sections of bilayers, whereas large length-scale assemblies of lamellar phases may be disallowed. Increased solution energy (via heating and sonication) may also allow for the generation of nano-sized vesicles that would otherwise be energetically unfavourable at the meso-scale for a given diblock copolymer composition; upon solution cooling, increased interchain packing may augment stabilization of the bilayered membrane, yielding the final nanoscale structure. The difference between assemblies at different length scales should, thus, be systematically explored for different diblock formulations of a given composition in order to determine if this is a universal effect or one that is dependent on polymer chain flexibility and diblock copolymer transition temperatures. In any event, this work demonstrates clearly that if nanoscale vesicles are the targeted design, there is no substitute for direct screening and characterization of diblock polymer compositions that give rise to self-assembled nanoscale morphologies via cryo-TEM.

Conclusions

A series of PEO-*b*-PCL diblock copolymers varying in PEO block size (M_n: 750, 1100, 2000 and 5000), f_{PEO} (0.08 – 0.33), and M_n (3.6 – 57K) were synthesized by ring-opening polymerization of ε-CL monomer using commercially available MePEO as the macro-initiator; anionic living polymerization was also employed to synthesize PEO-*b*-PCL copolymers with a wider range of controlled PEO block sizes (M_n: 1500, 2600, 3000, 3800, and 5800), f_{PEO} (0.10 – 0.23), and M_w (ranging from 7.8 to 47K). All copolymers were analysed by GPC and possessed narrow molecular weight distributions (PDI: 1.14 – 1.37).

The nature of the self-assembled aqueous morphologies derived from these polymers was probed on the micron scale using epifluorescent optical and scanning confocal fluorescence microscopies, and on the nanoscale via cryogenic transmission electron microscopy (cryo-TEM). Key morphological differences were observed to exist between self-assembled meso- and nanoscale structures for a given PEO-*b*-PCL diblock copolymer. While a single composition [PEO(2K)-*b*-PCL(12K); PDI = 1.21] provided self-assembled micron-sized structures in which vesicles were the most prevalently observed morphology under thin-film rehydration conditions, corresponding nanoscale polymersomes were formed from a multiplicity of PEO-*b*-PCL diblock copolymer compositions: these included PEO-*b*-PCL copolymers having a wide range of PEO weight fractions (f_{PEO}: 0.1 – 0.27), as well as PCL molecular weights (3.65 – 26K).

This work shows, for the first time, that morphological differences exist between self-assembled meso- and nanoscale structures for a given PEO-*b*-PCL diblock copolymer and underscores that PEO-*b*-PCL diblock copolymer compositions that form meso-scale polymersomes provide only limited insight into the distribution of PEO-*b*-PCL diblocks that give rise to corresponding vesicles on the nanoscale. Because PEO and PCL are FDA-approved polymers, this broad range of polymersome-forming PEO-*b*-PCL compositions suggests a more extensive utility of these species as nanometric drug delivery vehicles, as polymersomal bilayer thicknesses will undoubtedly modulate timescales of vesicle

degradation and corresponding release of polymersomal contents in biologically relevant applications.

Supplementary Material

Refer to Web version on PubMed Central for supplementary material.

Acknowledgments

This work was supported by grants from the Department of Defense (W81XWH-13-1-0086), the National Cancer Institute (R01CA115229), and the National Institutes of Health (EB003457-01). M.J.T. and D.A.H. thank the MRSEC Program of the National Science Foundation (DMR-00-79909) for infrastructural support.

Notes and references

1. Discher BM, Won YY, Ege DS, Lee J, Bates FS, Discher DE, Hammer DA. Science. 1999; 284:1143. [PubMed: 10325219]
2. Lee JCM, Bermudez H, Discher BM, Sheehan MA, Won Y-Y, Bates FS, Discher DE. Biotechnol. Bioeng. 2001; 73:135–145. [PubMed: 11255161]
3. Discher DE, Eisenberg A. Science. 2002; 297:967–973. [PubMed: 12169723]
4. Bermudez H, Brannan AK, Hammer DA, Bates FS, Discher DE. Macromolecules. 2002; 35:8203–8208.
5. Ghoroghchian PP, Frail PR, Susumu K, Blessington D, Brannan AK, Bates FS, Chance B, Hammer DA, Therien MJ. PNAS. 2005; 102:2922–2927. [PubMed: 15708979]
6. Ghoroghchian PP, Frail PR, Susumu K, Park TH, Wu SP, Uyeda HT, Hammer DA, Therien MJ. J. Am. Chem. Soc. 2005; 127:15388–15390. [PubMed: 16262400]
7. Ghoroghchian PP, Lin JJ, Brannan AK, Frail PR, Bates FS, Therien MJ, Hammer DA. Soft Matter. 2006; 2:973–980.
8. Ghoroghchian PP, Frail PR, Li G, Zupancich JA, Bates FS, Hammer DA, Therien MJ. Chem. Mater. 2007; 19:1309–1318. [PubMed: 19079789]
9. Duncan TV, Ghoroghchian PP, Rubtsov IV, Hammer DA, Therien MJ. J. Am. Chem. Soc. 2008; 130:9773–9784. [PubMed: 18611010]
10. Meng F, Engbers GHM, Feijen J. J. Controlled Release. 2005; 101:187–198.
11. Yu K, Zhang L, Eisenberg A. Langmuir. 1996; 12:5980–5984.
12. Yu K, Eisenberg A. Macromolecules. 1996; 29:6359–6361.
13. Yu K, Eisenberg A. Macromolecules. 1998; 31:3509–3518.
14. Shen H, Eisenberg A. Macromolecules. 2000; 33:2561–2572.
15. Ahmed F, Photos PJ, Discher DE. Drug Dev. Res. 2006; 67:4–14.
16. Christian DA, Cai S, Bowen DM, Kim Y, Pajerowski JD, Discher DE. Eur. J. Pharm. Biopharm. 2009; 71:463–474. [PubMed: 18977437]
17. Onaca O, Enea R, Hughes DW, Meier W. Macromol. Biosci. 2009; 9:129–139. [PubMed: 19107717]
18. Lomas H, Du J, Canton I, Madsen J, Warren N, Armes SP, Lewis AL, Battaglia G. Macromol. Biosci. 2010; 10:513–530. [PubMed: 20491130]
19. Murdoch C, Reeves KJ, Hearnden V, Colley H, Massignani M, Canton I, Madsen J, Blanazs A, Armes SP, Lewis AL. Nanomedicine. 2010; 5:1025–1036. [PubMed: 20874018]
20. van Dongen SFM, Nallani M, Schoffelen S, Cornelissen JJLM, Nolte RJM, van Hest J. Macromol. Rapid Commun. 2008; 29:321–325.
21. Kuiper SM, Nallani M, Vriezema DM, Cornelissen JJLM, van Hest JCM, Nolte RJM, Rowan AE. Org. Biomol. Chem. 2008; 6:4315–4318. [PubMed: 19005589]
22. Nallani M, Woestenenk R, de Hoog H-PM, van Dongen SFM, Boezeman J, Cornelissen JJLM, Nolte RJM, van Hest JCM. Small. 2009; 5:1138–1143. [PubMed: 19235803]
23. Fu Z, Ochsner MA, de Hoog HPM, Tomczak N, Nallani M. Chem. Commun. 2011

24. Meng F, Hiemstra C, Engbers GHM, Feijen J. Macromolecules. 2003; 36:3004–3006.
25. Adams DJ, Kitchen C, Adams S, Furzeland S, Atkins D, Schuetz P, Fernyhough CM, Tzokova N, Ryan AJ, Butler MF. Soft Matter. 2009; 5:3086–3096.
26. Johnston A, Dalton P, Newman T. J. Nanopart. Res. 2010; 12:1997–2001.
27. Ghoroghchian PP, Li G, Levine DH, Davis KP, Bates FS, Hammer DA, Therien MJ. Macromolecules. 2006; 39:1673–1675. [PubMed: 20975926]
28. Ahmed F, Hategan A, Discher DE, Discher BM. Langmuir. 2003; 19:6505–6511.
29. Ahmed F, Discher DE. J. Controlled Release. 2004; 96:37–53.
30. Bei J-Z, Li J-M, Wang Z-F, Le J-C, Wang S-G. Polym. Adv. Technol. 1997; 8:693–696.
31. Najafi F, Sarbolouki MN. Biomaterials. 2003; 24:1175–1182. [PubMed: 12527258]
32. Bellomo EG, Wyrsta MD, Pakstis L, Pochan DJ, Deming TJ. Nat. Mater. 2004; 3:244–248. [PubMed: 15034560]
33. Schuetz P, Greenall MJ, Bent J, Furzeland S, Atkins D, Butler MF, McLeish TCB, Buzza DMA. Soft Matter. 2011; 7:749–759.
34. Harashima H, Kiwada H. Adv. Drug Delivery Rev. 1996; 19:425–444.
35. Ueda I, Chiou J-S, Krishna PR, Kamaya H. BBA - Biomembranes. 1994; 1190:421–429. [PubMed: 8142445]
36. Drummond DC, Meyer O, Hong K, Kirpotin DB, Papahadjopoulos D. Pharmacol. Rev. 1999; 51:691. [PubMed: 10581328]
37. Florence AT, Hussain N. Adv. Drug Delivery Rev. 2001; 50:S69–S89.
38. Sass W, Dreyer HP, Seifert J. Am. J. Gastroenterol. 1990; 85:255–260. [PubMed: 2309677]
39. Jenkins PG, Howard KA, Blackball NW, Thomas NW, Davis SS, O'Hagan DT. J. Controlled Release. 1994; 29:339–350.
40. Bogdanov B, Vidts A, Van Den Buicke A, Verbeeck R, Schacht E. Polymer. 1998; 39:1631–1636.
41. J. J. Zastre J, Bajwa M, Liggins R, Iqbal F, Burt H. Eur. J. Pharm. Biopharm. 2002; 54:299–309. [PubMed: 12445560]
42. Hsu S-H, Tang C-M, Lin CCC-C. Biomaterials. 2004; 25:5593–5601. [PubMed: 15159075]
43. Cerrai P, Tricoli M, Andruzzi F, Paci M, Paci M. Polymer. 1989; 30:338–343.
44. Jeong Y-I, Kang M-K, Sun H-S, Kang S-S, Kim H-W, Moon K-S, Lee K-J, Kim S-H, Jung S. Int. J. Pharm. 2004; 273:95–107. [PubMed: 15010134]
45. Kricheldorf HR, Boettcher C, Tönnes K-U. Polymer. 1992; 33:2817–2824.
46. Schwach G, Coudane J, Engel R, Vert M. J. Polym. Sci., Part A: Polym. Chem. 2000; 35:3431–3440.
47. Kowalski A, Duda A, Penczek S. Macromolecules. 2000; 33:7359–7370.
48. Dong C-M, Qiu K-Y, Gu Z-W, Feng X-D. Macromolecules. 2001; 34:4691–4696.
49. Cammas S, Nagasaki Y, Kataoka K. Bioconjugate Chem. 1995; 6:226–230.
50. Nagasaki Y, Iijima M, Kato M, Kataoka K. Bioconjugate Chem. 1995; 6:702–704.
51. Hillmyer MA, Bates FS. Macromolecules. 1996; 29:6994–7002.
52. Deng M, Wang R, Rong G, Sun J, Zhang X, Chen X, Jing X. Biomaterials. 2004; 25:3553–3558. [PubMed: 15020129]
53. Rajagopal K, Mahmud A, Christian DA, Pajerowski JD, Brown AEX, Loverde SM, Discher DE. Macromolecules. 2010; 43:9736–9746. [PubMed: 21499509]
54. Photos PJ, Bacakova L, Discher B, Bates FS, Discher DE. J. Controlled Release. 2003; 90:323–334.
55. Zupancich JA, Bates FS, Hillmyer MA. Macromolecules. 2006; 39:4286–4288.
56. Sanson C, Schatz C, Le Meins J-F, Brulet A, Soum A, Lecommandoux S. Langmuir. 2009; 26:2751–2760. [PubMed: 19791794]
57. Jain S, Bates FS. Science. 2003; 300:460–464. [PubMed: 12702869]

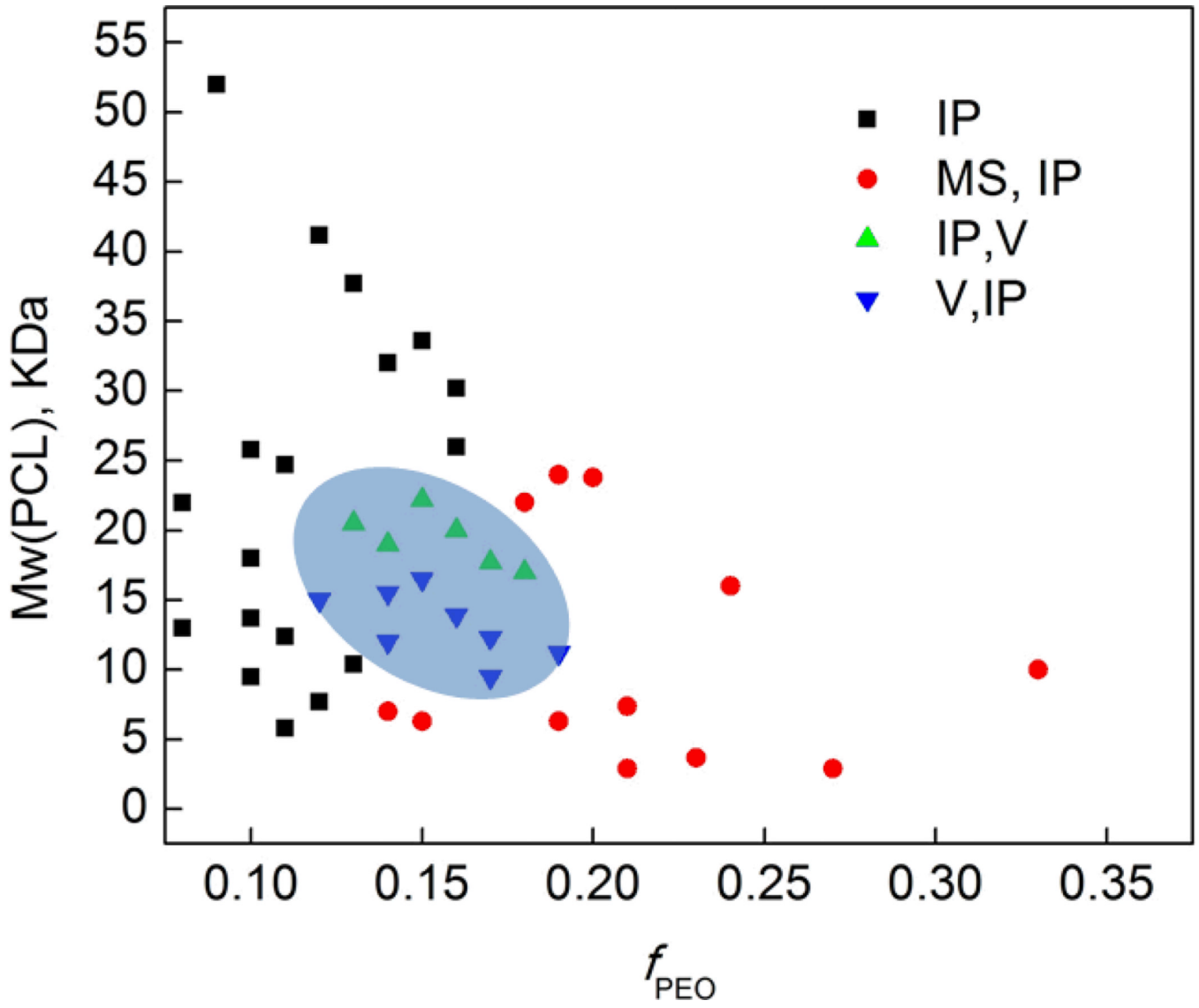

Fig. 1.

Phase diagram of micron-sized particles derived from aqueous hydration of PEO-*b*-PCL copolymers. Morphologies were determined qualitatively from fluorescence confocal microscopic studies of the self-assembled structures formed from thin film rehydration of 50:1 molar ratios of copolymer:Nile Red. Observed polymersome and irregularly shaped particle (IP) diameters ranged from less than 1 μm to greater than 30 μm; microsphere (MS) diameters ranged from ~5 – 30 μm; vesicles (V) diameters spanned ~5 – 50 μm. For systems exhibiting mixed morphologies, the major component is reported first.

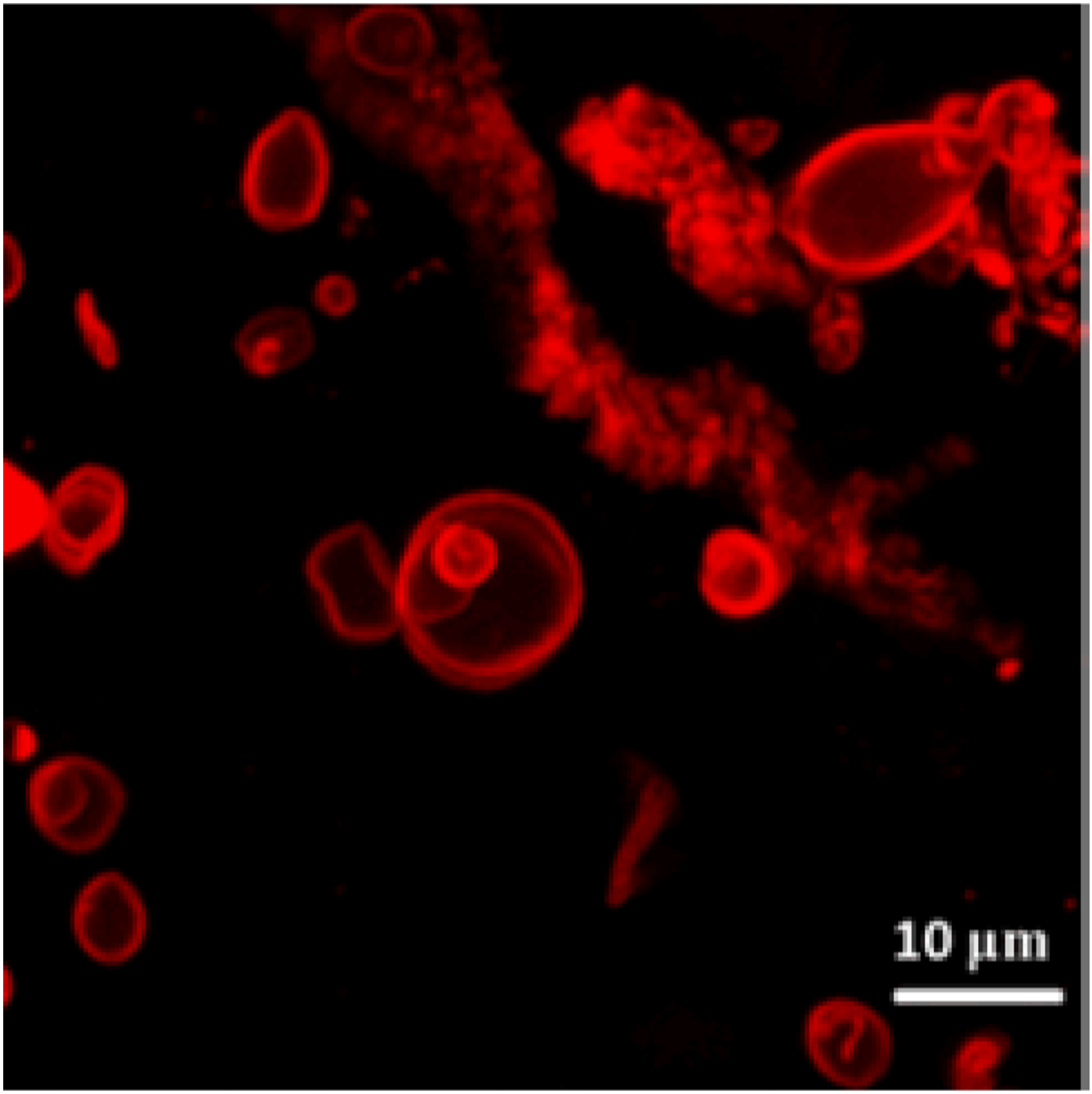

Fig. 2.

Scanning fluorescence confocal micrograph (λ_{ex} = 488 nm) of polymersomes derived from a 1:1:1 mixture of PEO(2k)-*b*-PCL(9.5k), PEO(2k)-*b*-PCL(12k), and PEO(2k)-*b*-PCL(15k), containing membrane-encapsulated Nile Red (peak emission = 603 nm) in DI water at 25 °C.

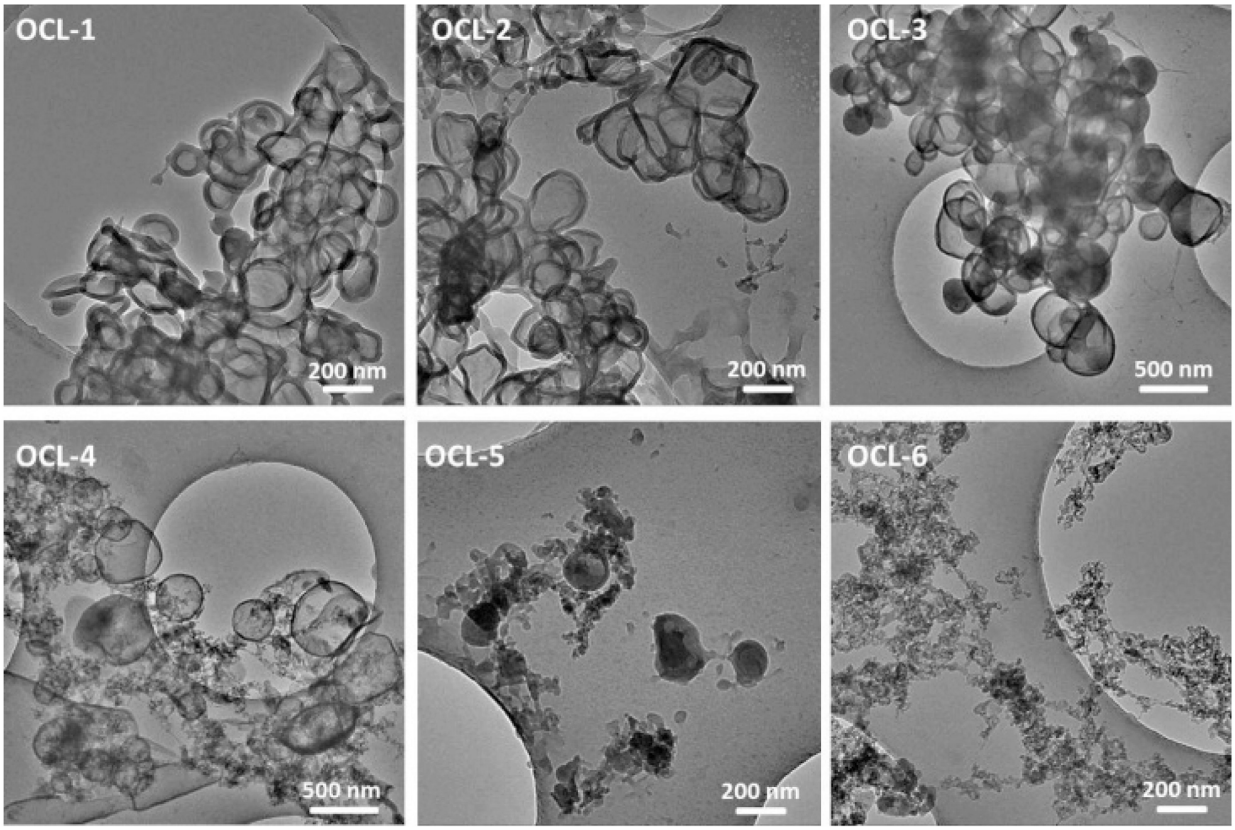

diblock copolymers with varying PEO block size (2.6K, 3K or

	OCL Copolymers	f_{PEO}	Extent to which vesicles comprise the visually observed morphologies
OCL-1	PEO(2K)-b-PCL(7.4K)	0.21	D
OCL-2	PEO(2K)-b-PCL(9.5K)	0.17	D
OCL-3	PEO(2K)-b-PCL(12K)	0.14	D
OCL-4	PEO(2K)-b-PCL(15K)	0.12	C
OCL-5	PEO(2K)-b-PCL(18K)	0.10	A
OCL-6	PEO(2K)-b-PCL(22K)	0.08	None

Fig. 3.

Cryo-TEM images of nanoscale polymersomes derived from PEO-*b*-PCL (OCL) diblock copolymers. Aqueous suspensions of OCL 1–6 were generated via thin-film hydration and subsequent self-assembly. D (dominant morphology): vesicles define the most prevalently observed morphological structure; C (common morphology): vesicles define one of the commonly observed morphological structures; A (atypical morphology): vesicles are observed, but such structures are less common than other observed morphologies.

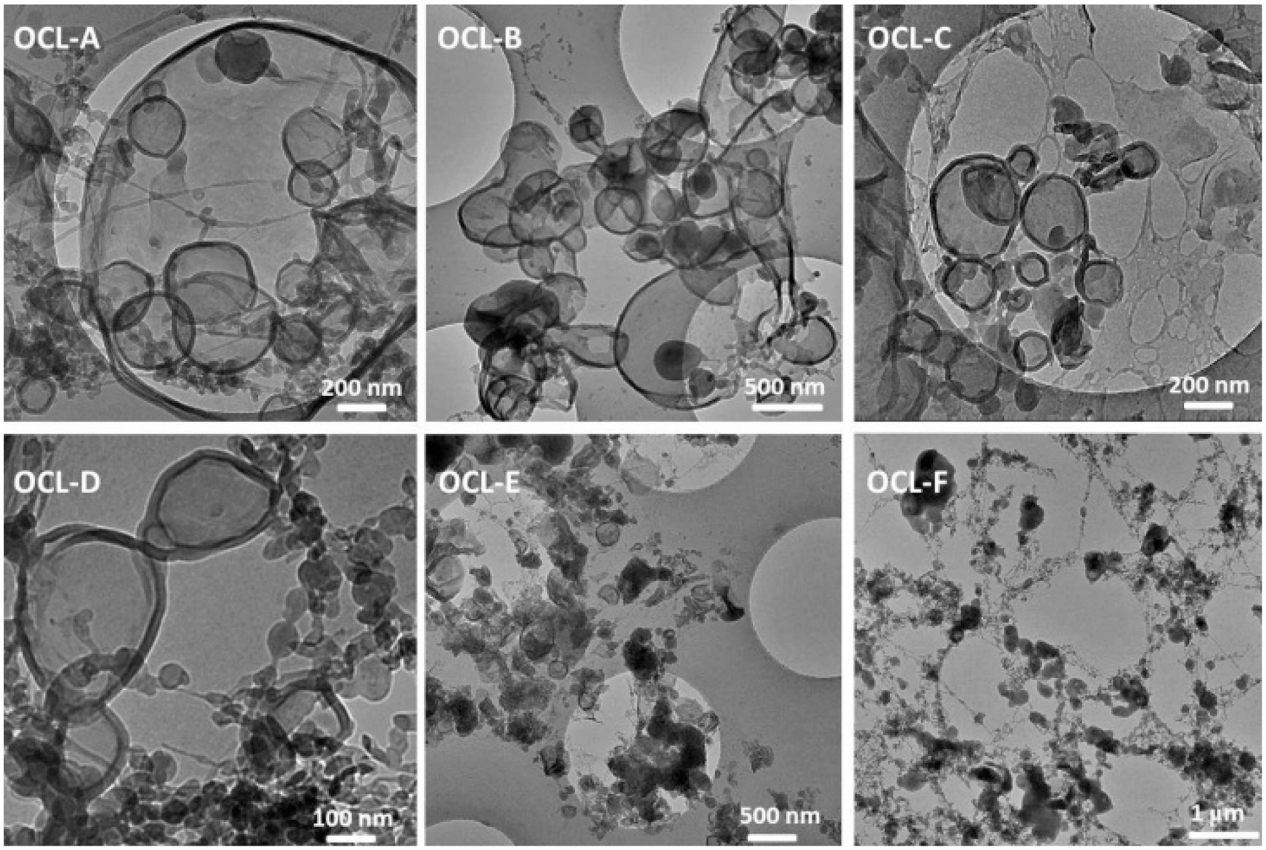

	OCL Copolymers	f_{PEO}	Extent to which vesicles comprise the visually observed morphologies
OCL-A	PEO(1.1K)-*b*-PCL(6.3K)	0.15	D
OCL-B	PEO(2K)-*b*-PCL(12K)	0.14	D
OCL-C	PEO(2.6K)-*b*-PCL(15.5K)	0.14	D
OCL-D	PEO(3K)-*b*-PCL(16.5K)	0.15	C
OCL-E	PEO(3.8K)-*b*-PCL(22.2K)	0.15	A
OCL-F	PEO(5K)-*b*-PCL(27K)	0.15	A

Fig. 4.

Cryo-TEM images of nanoscale polymersomes derived from PEO-b-PCL (OCL) diblock copolymers. Aqueous suspensions of OCL A–F were generated via thin-film hydration and subsequent self-assembly. D (dominant morphology): vesicles define the most prevalently observed morphological structure; C (common morphology): vesicles define one of the commonly observed morphological structures; A (atypical morphology): vesicles are observed, but such structures are less common than other observed morphologies.

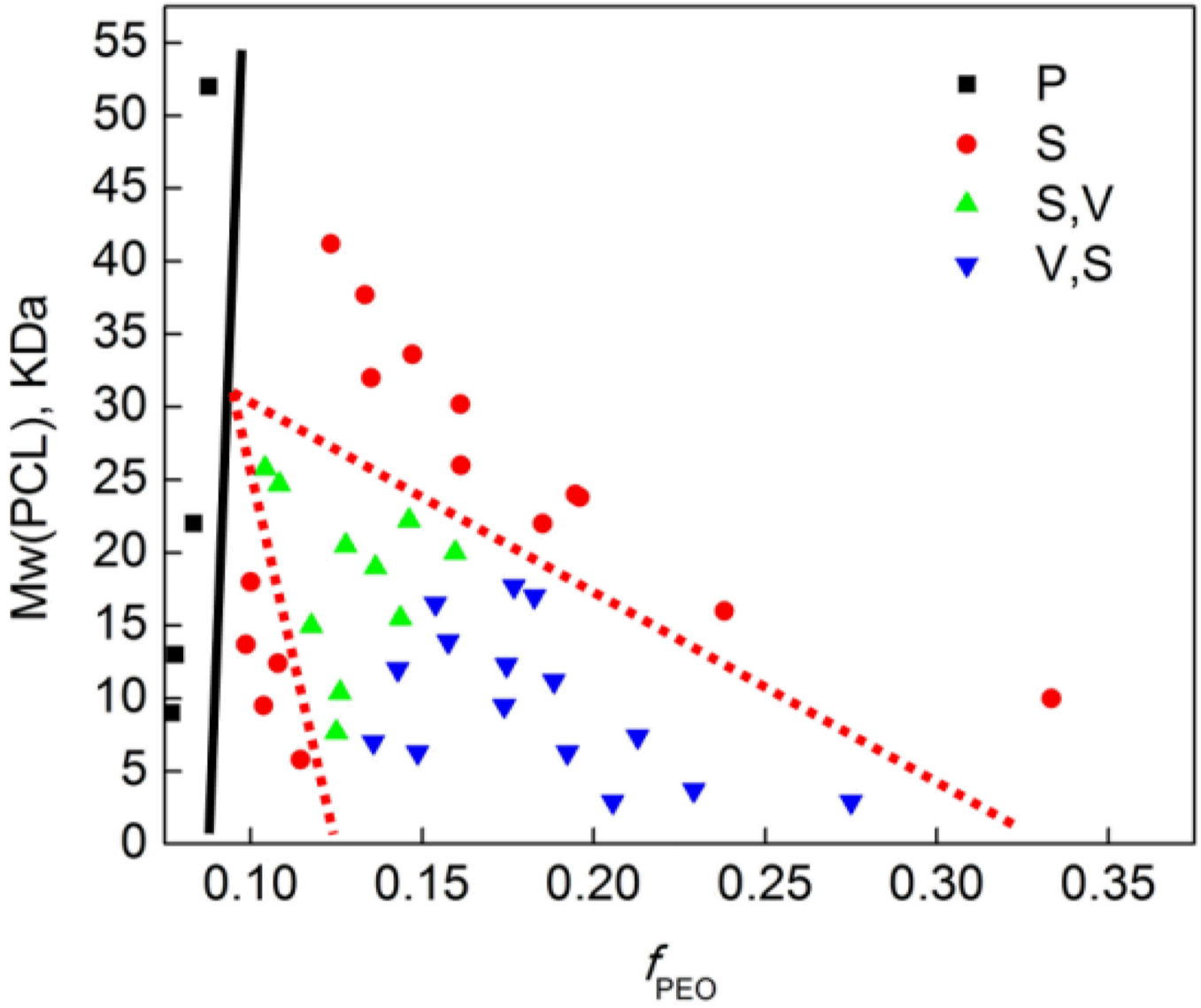

Fig. 5.

Phase diagram of nanoscale particles derived from aqueous hydration of PEO-*b*-PCL copolymers. Morphologies were determined qualitatively from cryogenic transmission electron microscopic studies of the self-assembled structures formed from thin film rehydration of 50:1 molar ratios of copolymer:Nile Red followed by extrusion through a 400 nm porosity membrane (S = spherical micelles, V = vesicle, P = precipitate; for systems exhibiting mixed morphologies, the major component is noted first).

Table 1

Comparative Self-Assembled Meso-Scale Morphologies of PEO-*b*-PCL Diblock Copolymers (PEO: 0.75 – 5.8K) Prepared via Thin-Film Hydration and their Corresponding Nanoscale Morphologies Observed in Aqueous Suspension

PEO-*b*-PCL Copolymers[a]	*f*PEO[b]	μm-Morphology[c]	nm-Morphology[d]
PEO(0.75K)-*b*-PCL(2.9K)	0.21	MS,IP	V,S
PEO(0.75K)-*b*-PCL(5.8K)	0.11	IP	S
PEO(0.75K)-*b*-PCL(9K)	0.07	IP	P
PEO(1.1K)-*b*-PCL(2.9K)	0.27	MS, IP	V,S
PEO(1.1K)-*b*-PCL(3.7K)	0.23	MS, IP	V,S
PEO(1.1K)-*b*-PCL(6.3K)	0.15	MS, IP	V,S
PEO(1.1K)-*b*-PCL(7.0K)	0.14	IP,MS	V,S
PEO(1.1K)-*b*-PCL(7.7K)	0.12	IP	S,V
PEO(1.1K)-*b*-PCL(9.5K)	0.1	IP	S
PEO(1.1K)-*b*-PCL(13.0K)	0.08	IP	P
PEO(1.5K)-*b*-PCL(6.3K)	0.19	MS, IP	V,S
PEO(1.5K)-*b*-PCL(10.4K)	0.13	IP	S,V
PEO(1.5K)-*b*-PCL(12.4K)	0.11	IP	S
PEO(1.5K)-*b*-PCL(13.7K)	0.1	IP	S
PEO(2K)-*b*-PCL(7.4K)	0.21	IP,MS	V,S
PEO(2K)-*b*-PCL(9.5K)	0.17	V,IP	V,S
PEO(2K)-*b*-PCL(12K)	0.14	V,IP	V,S
PEO(2K)-b-PCL(15K)	0.12	IP,V	S,V
PEO(2k)-b-PCL(18k)	0.1	IP	S,V
PEO(2K)-b-PCL(22K)	0.08	IP	P
PEO(2.6K)-b-PCL(11.2K)	0.19	V, IP	V,S
PEO(2.6K)-b-PCL(12.3K)	0.17	IP,V	V,S
PEO(2.6K)-b-PCL(13.9K)	0.16	IP,V	V,S
PEO(2.6K)-b-PCL(15.5K)	0.14	IP,V	S,V
PEO(3K)-b-PCL(16.5K)	0.15	IP,V	V,S
PEO(3K)-b-PCL(19K)	0.14	IP,V	S,V
PEO(3K)-b-PCL(20.5K)	0.13	IP,V	S,V
PEO(3K)-b-PCL(24.7K)	0.11	IP	S,P
PEO(3K)-b-PCL(25.8K)	0.1	IP	S,P
PEO(3.8K)-b-PCL(17K)	0.18	IP,V	V,S
PEO(3.8K)-b-PCL(17.7K)	0.17	IP,V	V,S
PEO(3.8K)-b-PCL(20K)	0.16	IP,V	S,V
PEO(3.8K)-b-PCL(22.2K)	0.15	IP,V	S,V
PEO(5K)-b-PCL(10K)	0.33	MS,IP	S
PEO(5K)-b-PCL(16K)	0.24	MS,IP	S
PEO(5K)-b-PCL(22K)	0.18	IP	S
PEO(5K)-b-PCL(26K)	0.16	IP	S

PEO-*b*-PCL Copolymers[a]	*f*PEO[b]	μm-Morphology[c]	nm-Morphology[d]
PEO(5K)-b-PCL(32K)	0.14	IP	S,P
PEO(5K)-b-PCL(52K)	0.09	IP	P
PEO(5.8K)-b-PCL(23.8K)	0.2	MS,IP	S
PEO(5.8K)-b-PCL(24K)	0.19	MS,IP	S
PEO(5.8K)-b-PCL(30.2K)	0.16	IP	S
PEO(5.8K)-b-PCL(33.6K)	0.15	IP	S
PEO(5.8K)-b-PCL(37.7K)	0.13	IP	S,P
PEO(5.8K)-b-PCL(41.2K)	0.12	IP	S,P

[a] Number-average molecular weight of PEO-b-PCL diblock copolymers as determined by ^{1}H NMR spectroscopy.

[b] Weight fraction of the PEO block as determined by ^{1}H NMR data.

[c] Morphology of particles determined qualitatively from fluorescence confocal microscopic studies of the self-assembled structures formed from thin-film rehydration of 50:1 molar ratios of copolymer: Nile Red. Observed polymersome and irregularly shaped particle (IP) diameters ranged from less than 1 μm to greater than 30 μm; microsphere (MS) diameters ranged from ~5 – 30 μm; vesicle (V) diameters spanned ~5 – 50 μm. In the cases of mixed morphologies, the major component is reported first.

[d] Morphologies of particles determined qualitatively from cryogenic transmission electron microscopic studies of the self-assembled structures formed from thin-film rehydration of 50:1 molar ratios of copolymer: Nile Red followed by extrusion through a 400 nm porous membrane (S = spherical micelles, V = vesicle, P = precipitate; for systems exhibiting mixed morphologies, the majority component is reported first). See Tables S3–4.